International Journal of Life science and Pharma Research
Content Available at www.ijlpr.com ISSN: 2250-0480

Molecular Docking Studies of Methanol Seed Fractions of Buchholzia Coriacea GC-MS Identified Compounds via Experimental and Computational Models

Okere Osheke Shekins[1], AmehDanladi Amodu[2], Nzelibe Humphrey Chukwuemeka[2], Bala M Shuaibu[2]

[1]*Department of Biochemistry, Bingham University, Karu, Nasarawa, Nigeria.*
[2]*Department of Biochemistry, Ahmadu Bello University, Zaria, Kaduna, Nigeria*

Article History: Received: 04.June.2025 Revised: 17.July.2025 Accepted: 18.Aug.2025

Abstract

This study aimed to examine the molecular docking studies of methanol seed fractions of Buchholzia coriacea GCMS identified compounds against target compoundprotein structurevia experimental and computational models. This study identified the active sites, as well as the functional groups (Methane isocyanato, xylene) in the α-amylase and α-glucosidase enzymes which were competitively inhibited. The mode of inhibition of in vitro α-amylase and α-glucosidase activity on the carbohydrate metabolizing enzymes was established to be competitive inhibition. The result of the oxidative stress enzyme shows that, there was a significant decrease ($p<0.05$) in super oxide dismutase (SOD), catalase (CAT), reduced glutathione (GSH) and a significant increase ($p>0.05$) in TBARS in diabetic rats when compared with normal and extract treated rats. A closer look at the results of the carbohydrate metabolizing enzymes shows that there was a significant increase ($p>0.05$) in Hexokinase, Phosphofructokinase (PFK), Glucose-6-phosphataseand Liver glycogen. When looking at the kidney function indices, the results reveal that there was a significant decrease ($p<0.05$) in Serum creatinine, Serum Urea and Serum Albumin, when compared with the diabetic control and extract treated Rats. Molecular docking of GC-MS-identified phyto-compounds from Buchholzia coriacea methanol seed fractions demonstrates strong binding potential to target proteins, supporting their therapeutic relevance. These findings, validated through experimental and computational models, highlight the plant's promise for future drug development.

Keywords: Experimental model,Computational model, Molecular Docking, Buchholzia coriacea, GC-MS.

***Corresponding Author**
Okere Osheke Shekins
Department of Biochemistry, Bingham University,
Karu, Nasarawa, Nigeria

DOI: https://doi.org/10.22376/ijlpr.v15i3.2010

INTRODUCTION

Plants contain a vast array of phytochemicals that are not just essential to them but also beneficial to man. These phytochemicals are frequently produced as defenses against harsh environmental conditions, prey, pests, and diseases [1]. These phytochemicals are plant secondary metabolites that validate the use of plants as natural therapies [2].

Buchholzia coriacea belongs to the family capparidacea and is widely distributed in several tropical countries [3]. The seeds of B. coriacea have medicinal value and this gave the plant a common name 'wonderful kola nut' because of its usage in traditional medicine to treat a variety of illnesses. The seeds or kernels of the plant *B. coriacea* are edible (can be eaten raw or cooked) and they have a spicy taste [4]. Scientific research on different parts of the plant has revealed various medicinal properties such as antihelmintic [5], antibacterial [6], antimicrobial [7], hypoglycemic [8, 9], antiplasmodial [10], antidiarhoeal and antispasmodic [4] and analgesic effects [11].

Polyphenols are an important group of phytochemicals that comprise stilbenes, coumarins, tannins, flavonoids, phenolic acids, and lignans. Phenolic acids represent benzoic and cinnamic acid derivatives [12].

According to estimates from the Global Burden of Diseases, Injuries, and Risk Factors Study [13], diabetes was the eighth leading cause of death and disability combined in the world, with nearly 460 million people across every country and age group living with the disease in 2019. Diabetes represents a substantial burden to health-care systems, [14] with estimates by the International Diabetes Federation (IDF) indicating that 537 million people worldwide had diabetes in 2021, resulting in health expenditures of US$966 billion globally, forecast to reach more than US$1054 billion by 2045 [15, 16]. The latest and most

comprehensive calculations show the current global prevalence rate of diabetes mellitus is at 6.1%, making diabetes one of the top 10 leading causes of death and disability [17].

In the field of molecular modeling, docking is a method which predicts the preferred orientation of one molecule to a second when a ligand and a target are bound to each other to form a stable complex[*18*]. Knowledge of the preferred orientation in turn may be used to predict the strength of association or binding affinity between two molecules using, for example, scoring functions.

The retrieval of protein structures was from the Protein Data Bank (http://www.rcsb.org) for the deposited three-dimensional structures of *human* α-amylase (HPA) complexed with acarbose (PDBID: 1B2Y), *human* α-glucosidase complexed with acarbose (PDB ID: 3TOP) and the pancreatic lipase co-lipase complex inhibited by an alkyl phosphonate (MUP901) (PDBID: 1LPB). The existing ligands and water molecules were removed from all the crystal structures while missing hydrogen atoms were added using MGL-AutoDock Tools (ADT, v1.5.6) [19].

This study aims to investigate the therapeutic effect of *Buchholzia coriacea* seed fractions on oxidative stress, carbohydrate metabolizing enzymes and kidney function indices via an experimental and computational approach.

MATERIALS AND METHODS

Plant material and preparation of extracts

Fresh (seed) samples of *Buchholzia coriacea* (*Engl*) were purchased from Kafanchan market in Kaduna State and identified at the Department of Biology of the Faculty of Life Sciences, Ahmadu Bello University, Zaria (ABU Zaria). After immediately cleaning the seeds of debris, they were peeled, chopped, and allowed to dry in the shade (1 week) in laboratory trays. The seeds were then weighed and ground into a powder from which 2200g was then separated into two equal portions and macerated in (3000 ml) distilled water and methanol, respectively, and left for 48 hours, with intermittent shaking (every 6 hours) [20]. Following the 48-hour period, the sample mixture was filtered (Whatman's No. 1 filter paper). The extract was then obtained with a rotary evaporator. The solvent was extracted at a temperature of 45°C and pressure of 60mmHg of water. The paste-like extract was obtained and oven-dried to complete solid, then ground to smooth powdered form and stored in a refrigerator till use

Ligand Preparation

The retrieval of Structure Data Format (SDF) of reference inhibitors and the GCMS identified phyto-compounds from methanol seed fractions of *Buccholzia coriacea* were downloaded from the PubChem database (www.pubchem.ncbi.nlm.nih.gov). The compounds were further converted to the pdb chemical format by means of Open babel [21]. Non-polar hydrogen molecules were merged with the carbons, while the polar hydrogen charges of the Gasteiger-type were assigned to atoms. Furthermore, ligand molecules were converted to dockable PDBQT format with the help of AutoDock Tools.

Validation of Molecular Docking Protocol

To confirm the docking methodology to be utilised for the virtual screening, the extracted co-crystallized ligand from both proteins was aligned with the docked poses of the native ligands (acarbose) with the least binding affinity from the first docking. The RMSD was calculated using Discovery Studio Visualizer, BIOVIA, 2020.

Determination of Superoxide Dismutase

Superoxide dismutase (SOD) activity was determined using the method ofMisra and Fridovish [22]. The ability of enzymes to inhibit auto oxidization of catecholamine is the basis of the SOD assay. Three milliliters (3.0 mL) of reaction mixture contains 1.5 ml volume of buffer system (0.1Mcarbonate bicarbonate buffer; at pH 10.3), 0.1mlof 30mM EDTA, an appropriate amount of enzyme source and water to complete the volume to 2.94 ml while the reaction was initiated by the addition of 15mM epinephrine (0.06 ml volume). The absorbance change was recorded at 480nm for 1 min with an interval of 15s. Controls including all components, except enzyme preparations, were run concurrently.

$$\textbf{Increase in absorbance for substrate} = \frac{\textbf{ABS}_{60} - \textbf{ABS}_{15}}{2}$$

Where:

ABS_{15} = Absorbance after 15seconds

ABS_{60} = absorbance after 60seconds

$$\%\ \textbf{Inhibition} = 100 - \left(\frac{\textbf{Increase within the Absorbance of Substrate}}{\textbf{Increase within the Absorbance of Blank}}\right) \times 100$$

One unit of super oxide dismutase SOD activity was specified as the measure of SOD needed to bring about 50% inhibition of the oxidization of epinephrine. The unit of SOD activity is in the international unit (U/L).

$$\textbf{Specific enzyme activity} = \left(\frac{\textbf{Enzyme activity}}{\textbf{Total Protein Concentration}}\right)$$

Determination of Catalase Enzyme

Catalase (CAT) activity was spectrophotometrically determined at 510nm using themethod of Aebiusing BIODIAGNOSTIC Research and Reagent kit[23]. Four samples were set up labeled standard, standard blank, sample and sample blank respectively. Fifty microliters (0.05 ml) of the tissue homogenate was added to the tubes labeled sample blank and sample whereas 0.1ml each of hydrogen peroxide (diluted 1000 times by adding 10µl H_2O_2 to 10 ml distilled water) was added to the tubes labeled "sample" and "standard" whereas 0.1 ml of H_2O added to plain blank. Then 0.5ml of the phosphate buffer was added to each of the four tubes and incubated at room temperature for one minute. The reaction was completed by the addition of 0.2 ml of the chemical compound matter and 0.5 ml of the oxidase catalyst (HRP) into every tube followed by incubation for ten minutes at 37°C. The absorbance of the sample (A_{Sample}) was read against the sample blank

whereas the absorbance of standard ($A_{Standard}$) browsed against standard blank at 510nm. The enzyme activity within the tissue was calculated as:

$$Catalase\ Activity\ (U/g) = \frac{A_{Standard} - A_{Sample}}{A_{Standard}} \times \frac{1}{gm.\ of\ tissue\ used}$$

Where:
A_{Sample} = Absorbance of Sample – Absorbance of a Sample blank
$A_{Standard}$ = Absorbance of Standard – Absorbance of Sample blank

Determination of Reduced Glutathione

Determination of total reduced glutathione content was carried out according to the protocol of Ellmanbased on yellow colour development with maximum absorbance at 412 nm upon the reaction of 5,5'-dithio-2-nitro benzoic acid (DTNB) with sulfhydryl group containing compounds[24].Half milliliter (0.5ml) of tissue homogenate in phosphate buffer was deproteinized and precipitated in 2ml of 5% trichloroacetic acid (TCA) and centrifuged. Ellman reagent (0.5ml) was added to 1ml of the supernatant after centrifugation and 3 ml of phosphate buffer added which led to development of yellow colour that was read at 412nm. An array of standards was treated similarly with a blank containing 3.5ml of phosphate buffer. The amount of glutathione is expressed in mM/g of wet tissue.

Determination of Liver and Kidney Thiobarbituric Acid Reacting Substances (TBARS) Level

The test is principled on the formation of a pink product from the reaction between Thiobarbituric acid reacting substances (TBARS) and thiobarbituric acid (TBA) whose colour intensity at 535nm is directly proportional to the TBARS in the sample [25].One milliliter of trichloroacetic acid (15%) was dosed into a test tube, followed by 1ml of thiobarbituric acid and 50µl of tissue homogenate. The mixture was incubated at 80°C for 30 minutes in a water bath and allowed to cool for 2min, then centrifuged at 1000xg for ten (10) minutes. The absorbance of the supernatant was clearly read at 535nm in a spectrophotometer. The TBARS concentration was estimated as follow:

$$TBARS\ Conc.\ (nmol/mg\ protein) = \frac{Sample\ Absorbance}{1.56 \times 10^{-5} \times Protein\ concentration}$$

Determination of Hepatic Hexokinase

Glucose-6-phosphateis produced in the conjugated hexokinase reaction withglucose-6 phosphate dehydrogenase. The reaction was followed by measuring the increase in absorbance at 340nm due to the formation of NADPH. Sufficient excess glucose-6-phosphate dehydrogenasewas provided to minimize transit time and avoid hexokinase inhibition by glucose-6-phosphate [26].To assay buffer (1.4 ml), 0.04 ml of enzyme source, 0.2 ml each of NADP (Nicotinamide adenine dinucleotide phosphate) and glucose-6-phosphate dehydrogenase were added and incubated for five minutes at 37°C. Initiation of the reaction through the addition of 0.2 ml ATP (Adenosine triphosphate) followed by the measurement of the increase in absorbance at one minute interval for five minutes at 340 nm using a spectrophotometer. The enzymatic activity was estimated using a NADPH extinction factor of $6.22cm^{-1}mmol^{-1}$and expressed as nanomoles of glucose-6-phosphate formed/min/mg protein.

Determination of Hepatic Glucose-6-Phosphatase

Glucose-6-phosphate was incubated with enzyme source in citrate buffer and therefore the reaction was in remission following the tactic of King [27]. The inorganic phosphate (Pi) liberated was calculable by the tactic of Fiske and Subbarow [28].Incubation of a mixture of glucose-6-phosphate (0.5ml), buffer (0.4ml) and enzyme source (0.1ml) was carried out at 37°C for one (1) hour, the reaction stopped upon addition of 10% trichloroacetic acid (TCA) while enzyme source was added after stopping the reaction. The resultant supernatant obtained upon centrifugation at 4000rpm for 15minutes was employed to estimate the amount of inorganic phosphate released [27]. Enzyme activity is expressed as the number of pmol Pi released/hour/mg protein.

Measurement of Serum Creatinine

Creatinine in a protein-free filtrate reacts with alkaline picrate to form a coloured complex, the absorbance of which is measured at 500-550 nm [29]. The creatinine working reagent was a freshly prepared mixture of saturated picric acid solution (10ml) and 10% Sodium hydroxide solution (2.0ml). Stock creatinine standard (10mmol/L) was prepared by dissolving 0.602g of creatinine zinc chloride and making up the volume to 100ml with 100mmol/L (0.1N) hydrochloric acid. This stock creatinine standard was further diluted 1:50 to 200µmol/L to produce the working creatinine standard. To two sets of three test tubes containing samples labeled B (for blank), S (for standard) and T (for test) containing 2.0ml of the working reagent; 0.2ml of distilled water, working creatinine standard (200µmol/L) and serum samples were added respectively, well mixed and left at room temperature for 90 minutes. The absorbances of the first set of tubes were read after setting the instrument to zero with the blank. Into the second set of tubes, 50µl (0.05ml) of 60% v/v acetic acid were added and left for 10 minutes. The instrument was set to zero with the blank of the second set of test tubes to get the second reading. The final reading was then obtained by subtracting the second reading from the first reading to eliminate the colour developed due to non- specific chromogens. The creatinine concentration in the samples was calculated as:

$$Creatinine\ (\mu mol/L) = \frac{Absorbance\ of\ Test}{Absorbance\ of\ Standard} \times 200$$

Measurement of Serum Urea

The Abnova Urea assay was used to estimate serum urea in this study according to the manufacturer's

instructions. Reagent A, Reagent B, Urea Standard (50mg/dL) and serum samples were equilibrated at room temperature. Equal volumes (10mL each) of Reagent A and Reagent B were freshly mixed just before the test so that the active reagent can be usedupwithin20 minutes of mixing. Incorrectly labeled tubes, 20µl of water, standard (50mg/dl) and samples were transferred. One thousand microliters (1000µl) of active reagent was added and lightly tapped to mix. The mixture was incubated for 20min and absorbance (ABS) was read at 520nm using a spectrophotometer. The concentration of urea in the samples was calculated by the formula:

$$\textbf{Urea conc. } (\textbf{mg/dl}) = \textbf{ Conc of Standard } \times \frac{\textbf{ABS}_{\textbf{Sample}} - \textbf{ABS}_{\textbf{Blank}}}{\textbf{ABS}_{\textbf{Standard}} - \textbf{ABS}_{\textbf{Blank}}} \times \textbf{n}$$

ABS_{Sample}, ABS_{Blank} and $ABS_{Standard}$ are optical density values of sample, water, and standard respectively.
n is the dilution factor.
Concentration of urea standard is 50mg/dl.
Conversions: BUN (mg/dl) = [Urea] / 2.14, and 1mg/dl Urea = mmol/L x 6.

Measurement of Serum Albumin

Bromocresolgreen, an anionic dye, binds tightly to albumin when added to serum and the complex absorbs light much more strongly at pH 4.2 and 628nm compared with unbound dyes. The increase in light absorption is proportional to albumin concentration [30]. Three test tubes were set up as "Test, Standard and Blank". The Test cocktail was made up of Bromocresol green (BCG) reagent (5.0ml) and serum (0.05ml) while the standard cocktail made up of BCG (5.0 ml) and 4% Albumin (0.05 ml, prepared by dissolving 4.0 g of bovine albumin in 100ml of normal saline) and the blank cocktail made up of blank reagent (5.0ml). The cocktails were well mixed, allowed to stand for 10minutes at room temperature after which the absorbance were read at 640nm, setting to zero with blank. The serum albumin concentration was obtained using the formula:

$$\frac{Absorbance\ of\ Test}{Absorbance\ of\ Standard} \times Conc\ of\ Standard = \frac{Absorbance\ of\ Test}{Absorbance\ of\ Standard} \times 4\ g/dl$$

MOLECULAR DOCKING OF GCMS IDENTIFIED COMPOUNDS

Molecular Docking of Phytochemicals with Targeted Active Site

The active site directed molecular docking of the reference inhibitors and the GCMS identified compounds against the three protein targets was performed using AutoDockVina in PyRx 0.8[31]. The ligands were imported for the docking study, and PyRx 0.8's Open Babel [21] was used to minimize energy. The energy minimization parameter and conjugate gradient descent used was the Universal Force Field (UFF) and optimization algorithm respectively. Although, other parameters not mentioned were set at default, the binding site coordinates of the target enzymes are presented in Table 3.1 and Discovery Studio Visualizer version 16 was used to view the molecular interactions.

Table0 1: Binding site coordinates of the target enzymes

Dimensions	**1b2y** (Å)	**3top** (Å)	**1LPB** (Å)
center_x	18.87	-31.87	8.00
center_y	6.13	35.49	24.34
center_z	47.10	26.65	54.26
Size x	22.08	21.63	18.53
Size y	23.46	23.29	21.53
Size z	20.47	20.98	20.98

RESULTS

Results for oxidative stress parameters for Buchholzia coriacea seed fraction

Induction of diabetes was found to significantly ($p<0.05$) lower the activity of the antioxidant markers; superoxide dismutase (SOD), catalase (CAT) and reduced glutathione (GSH) in the diabetic control group compared with the normal control. It was however noticed that the activity of the antioxidant markers which were significantly suppressed in the diabetic control was significantly ($p<0.05$) increased in the treated groups of n-hexane, n-butanol, ethyl acetate and aqueous fractions.

Table 02: Effect of *Buchholzia Coriacea* Seed Fractions on Oxidative Stress Parameters in Normal and STZ–Induced Diabetic Rats.

Group	**Super oxide dismutase (SOD) (U/mg of protein)**	**Catalase (CAT) (U/mg of protein)**	**Reduced glutathione (GSH) µmole/mg protein**	**TBARS (nMole/g tissue)**
Normal Control	6.43 ± 0.11^{a}	83.92 ± 2.06^{a}	41.65 ± 3.16^{a}	0.50 ± 0.03^{b}
Diabetic Control	2.43 ± 0.08^{d}	46.82 ± 1.10^{c}	22.46 ± 0.61^{c}	1.05 ± 0.06^{a}
Met 100mg/kg	4.25 ± 0.14^{c}	81.66 ± 1.63^{a}	42.86 ± 1.01^{a}	0.51 ± 0.03^{b}
nHex 100mg/kg	4.94 ± 0.12^{b}	80.11 ± 2.12^{a}	42.96 ± 0.98^{a}	0.52 ± 0.02^{b}

nBut 100mg/kg	4.67 ± 0.15[b]	80.64 ± 1.41[a]	42.31 ± 1.12[a]	0.60 ± 0.04[b]
EtoAc 100mg/kg	3.96 ± 0.18[c]	70.89 ± 2.48[b]	34.97 ± 1.05[b]	0.64 ± 0.08[b]
AFBC 100mg/kg	3.88 ± 0.11[c]	72.43 ± 3.45[b]	35.22 ± 0.91[b]	0.65 ± 0.06[b]

[a-e]Values expressed as Mean ± SEM of five animals. Values with different letters along the last column are significantly ($p<0.05$) different from each other.

Results for Carbohydrate Metabolizing Enzymes

The activities of glucose metabolizing enzymes like hexokinase, Phosphofructokinase, Glucose-6-phosphatase and liver glycogen were significantly ($p<0.05$) lowered in the liver of diabetic untreated rats. Hexokinase level were significantly ($p<0.05$) increased in the n-hexane, n-butanol, ethyl acetate and the aqueous treated groups when compared to the diabetic control.The result of the evaluation of PFK levels in the rats showed that there was a significant ($p<0.05$) increase among the n-hexane, n-butanol, ethyl acetate and aqueous treated groups when comparing them to the diabetic control, while evaluation of the G6Pase levels showed that there was a significant ($p<0.05$) increase among the n-butanol, ethyl acetate and aqueous treated groups when compared to the diabetic control.Evaluation of the liver glycogen levels showed that there was a significant ($p<0.05$) increase among the n-hexane, n-butanol, ethyl acetateand aqueous treated groups when compared to the diabetic control.

Table 03: Effect of *B. coriacea* seed fractions on carbohydrate metabolizing enzymes in normal and STZ-induced diabetic rats

Group	Hexokinase (mg/100ml)	Phosphofructokinase (PFK) (mMole/min/mg of protein)	Glucose-6-phosphatase (unit/mg protein)	Liver glycogen (mg/100mg of glucose)
Normal Control	12.20 ± 0.23[bc]	27.12 ± 0.93[d]	28.30 ± 0.79[d]	0.19 ± 0.03[a]
Diabetic Control	9.57 ± 0.45[c]	22.03 ± 0.47[e]	22.17 ± 0.61[e]	0.04 ± 0.00[c]
Met 100mg/kg	18.74 ± 0.24[abc]	29.70 ± 0.41[d]	29.70 ± 0.41[d]	0.16 ± 0.01[a]
nHex 100mg/kg	23.54 ± 0.46[ab]	33.87 ± 0.99[c]	34.89 ± 0.57[c]	0.17 ± 0.01[a]
nBut 100mg/kg	20.06 ± 0.24[abc]	41.38 ± 0.82[b]	43.07 ± 0.98[b]	0.15 ± 0.01[a]
EtoAc 100mg/kg	17.18 ± 1.08[abc]	38.93 ± 2.22[b]	43.62 ± 1.81[b]	0.10 ± 0.01[b]
AFBC 100mg/kg	30.55 ± 11.09[a]	48.18 ± 0.59[a]	46.82 ± 0.85[a]	0.10 ± 0.01[b]

Values are represented as Mean ± SEM. Values not sharing common letters are statistically different ($p<0.05$).

Results for kidney function indices

Table 04: Effect of *B. Coriacea* Seed Fractions on Kidney Function Indices in Normal and STZ-Induced Diabetic Rats

Group	Serum creatinine (mg/100ml)	Serum Urea (mg/100ml)	Serum Albumin (mg/100ml)
Normal Control	2.01 ± 0.21[b]	129.55 ± 4.28[b]	11.48 ± 1.13[bc]
Diabetic Control	9.58 ± 0.34[a]	191.44 ± 13.45[a]	19.46 ± 1.09[a]
Met 100mg/kg	2.29 ± 0.13[b]	123.00 ± 6.01[b]	9.29 ± 0.51[bc]
nHex 100mg/kg	2.17 ± 0.14[b]	140.19 ± 4.67[b]	10.69 ± 0.57[bc]
nBut 100mg/kg	2.13 ± 0.20[b]	123.57 ± 8.88[b]	11.05 ± 0.46[c]
EtoAc 100mg/kg	2.13 ± 0.15[b]	129.04 ± 12.06[b]	11.77 ± 0.51[b]
AFBC 100mg/kg	2.06 ± 0.17[b]	142.37 ± 8.55[b]	12.36 ± 0.32[b]

Values are represented as Mean ± SEM. Values not sharing common letters are statistically different ($p<0.05$)

The serum creatinine levels show clear elevation in the diabetic control group when compared with the n-hexane, n-butanol, ethyl acetate and aqueoustreated groups. The same holds true for the serum urea levels where the diabetic control group was significantly ($p<0.05$) higher than the n-hexane, n-butanol, ethyl acetate and aqueous treated groups. However, the opposite trend was observed in the serum albumin levels, as there was a significant ($p<0.05$) decrease in the serum albumin levels when comparing the diabetic control with the n-hexane, n-butanol, ethyl acetate and aqueous treated groups

Molecular docking of GCMS identified compounds from methanol seed fraction of Buccholzia coriacea against target proteins

The binding affinities from the docking analysis of the **GC-MS identified compounds** against these protein targets are shown in Table 4. Based on the minimum binding energies, binding poses and interaction in the catalytic site, the top two ranked compounds for each enzyme was selected for interactive analyis. After ranking, it was observed that the top two docked compounds to the 3 targets had multiple high binding tendencies.

Table 05: List of identified phytocompounds of methanol extract of *Buchholzia coriacea* seed

SN	RT(min)	Name of compound	Molecular Formula	Molecular Weight	Peak Area	Nature of Compound	Structure
1	5.2286	E-11-Hexadecenal	$C_{16}H_{30}O$	238.41	2.7595	Pherormone	
2	13.4339	Dodecanoic acid, methyl ester	$C_{13}H_{26}O$	214.34	0.4365	Fatty acid methyl ester	
3	13.8127	Heptadecanoic acid, 9-methyl-, methyl ester	$C_{19}H_{38}O_2$	298.29	1.5299	Fatty acid methyl ester	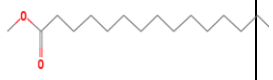
4	13.9968	Dodecanoic acid, methyl ester	$C_{13}H_{26}O_2$	214.34	0.7415	Fatty acid methyl ester	
5	15.727	pentanoic acid, 2,4,4-trimethyl-3-oxo-, methyl ester	$C_{11}H_{21}O_5P$	264.25	0.6349	Ester	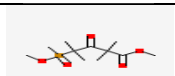
6	15.9171	9-Octadecenoic acid (Z)-, 3-[(1-oxohexadecyl)oxy]-2-[(1-oxooctadecyl)oxy]propyl ester	$C_{51}H_{98}O_6$	807.30	0.0229	Fatty acid propyl ester	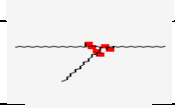
7	18.6655	Methyl tetradecanoate	$C_{15}H_{30}O_2$	242.40	2.2804	Fatty acid methyl ester	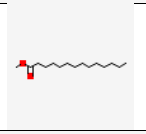
8	20.1784	Docosanoic acid, ethyl ester	$C_{24}H_{48}O_2$	368.64	1.1175	Ester	
9	22.9273	Hexadecanoic acid, methyl ester	$C_{17}H_{34}O_2$	270.45	9.2881	Fatty acid	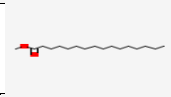
10	24.2923	Hexadecanoic acid, ethyl ester	$C_{18}H_{36}O_2$	284.48	32.9002	Fatty acid	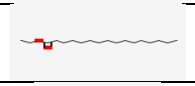
11	26.1901	9,12-Octadecadienoic acid, methyl ester	$C_{19}H_{34}O_2$	294.47	1.3901	Fatty acid	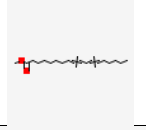
12	26.3178	9-Octadecenoic acid (Z)-, methyl ester	$C_{19}H_{36}O_2$	296.49	15.8181	Fatty acid methyl ester	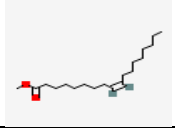

13	26.8385	Methyl stearate	$C_{19}H_{38}O_2$	298.50	2.3822	Fatty acid ester	
14	27.4412	Linoleic acid ethyl ester	$C_{20}H_{36}O_2$	308.51	1.5246	Fatty acid ethyl ester	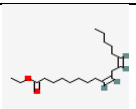
15	27.5661	Ethyl Oleate	$C_{20}H_{38}O_2$	310.51	25.9083	Fatty Acid ester	
16	28.0774	Octadecanoic acid, ethyl ester	$C_{20}H_{40}O_2$	312.53	2.1515	Fatty acid	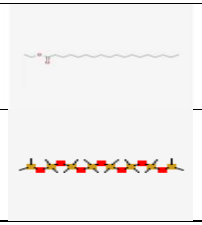
17	37.8163	Octasiloxane, 1,1,3,3,5,5,7,7,9,9,11,11,13,13,15,15-hexadecamethyl-	$C_{16}H_{48}O_7Si_8$	577.26	-1.2375	Silicon polymer	

Table 05: Binding energies of GCMS identified compounds from methanol seed fraction of *Buccholziacoriacea* against target proteins (1B2Y, 3TOP, 1LPB).

Ligand	**Binding Affinity (Kcal/mol)**		
	1b2y	**3top**	**1LPB**
Acarbose_1b2y (uff_E=376.73)	-15.9	-13.9	-
MUP901 (uff_E=-147.99)	-	-	-5.8
Methane_isocyanato- (uff_E=133.43)	-7.5	-8	-7.7
p_Xylene (uff_E=107.17)	-5.1	-5.7	-5.7
1,5-Hexadiyne (uff_E=5.33)	-4.1	-4.8	-4.3
o-Allylhydroxylamine_uff_E=41.05)	-3.8	-3.7	-3.5
Pyridine_2,3,45-tetrahydro (uff_E=74.62)	-3.7	-4.5	-3.8
Methylacrylonitrile (uff_E=8.71)	-3.5	-4.2	-3.5
1-Azabicyclo[3.1.0]hexane_uff_E=1593.69)	-3.4	-4.5	-3.6
2-Butanamine (uff_E=36.23)	-3.4	-3.8	-3.4
Pyrrole (uff_E=199.05)	-3.2	-3.8	-3.3
Propargylamine (uff_E=19.96)	-3	-3.5	-2.9
2-Propen-1-amine (uff_E=21.82)	-3	-3.3	-2.9
2-Propenal (uff_E=4.49)	-2.8	-3.2	-3
minoacetonitrile (uff_E=20.74)	-2.7	-3.1	-3
Ethenamine_N-methylene- (uff_E=7.55)	-2.7	-3	-2.7
Ethyl_isocyanide (uff_E=15.93)	-2.7	-3	-2.7
Chlorine_dioxide (uff_E=0.52)	-1.7	-1.4	-1.7

For the validation of the docking protocol, the co-crystallized reference compounds (acarbose) were docked into the binding site of the co-crystallized proteins with the binding energy of -13.9kcal/mol. The two top docked compounds Methane_isocyanato and p_Xylene presented binding energies of -7.5 and -5.1; -8 and -5.7 and -7.7 and -5.7 kcal/mol to 1B2Y, 3TOP and 1LPB.

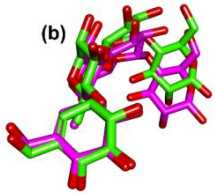

Figure 01:Superimposition of best docked conformer of the co-crytalized reference compound on the extracted conformation of acarbose.The green colour compounds represented the docked conformer, while the red and purple conformation represents the extracted conformation from 3top.

Amino acid interaction of top two docked GCMS identified phytochemical and reference compounds with the three protein targets

The majority of the interactions between the ligand groups and the enzyme residues were hydrophobic, with a small number of H-bonds below 3.40Å. From the validation analysis, in a similar binding conformation as the native ligand, acarbose was stretched in the long, narrow, hydrophobic gorge of 3TOP. Both Methane_isocyanato and Xylene made few hydrogen bonds and hydrophobic contacts with the catalytic residues at the hydrophobic gate of α-amylase which is composed of residues Trp-59, Tyr62, and His299 and other catalytic residues such as; Asp197, His305, Glu233, Arg197, and Ala198. The top docked phytochemicals were docked into the active sites of 3TOP in close fashion as the reference compound acarbose and interacted with catalytic residues as acarbose.

Table 06:Amino acid interaction of the top two docked GCMS identified phytochemicals from the docking analysis with the three target proteins.

Compounds	Protein	Hydrogen bonds	Hydrophobic Interaction
		Interacting residues	Interacting residues
MUP901	1LPB	Asp79 Phe77 Arg256	Phe215 His263 Tyr114 Pro180 Ile78
Methane isocyanato		Arg256	Phe215 Ala178 Tyr114 His263
p-Xylene			His263 Phe215 Tyr114 Pro180
Acarbose	1B2Y	Trp59 Gln63Tyr62 Thr163 GLy306 Thr163 His305 His299 Tyr62 Tyr151 His201 Lys200 Ile235 Arg195Asp197 Lys200 Glu233 Asp300	Trp59
Methane isocyanato		Gln63 Asp300	Ala198 Tyr62 Leu165
p-Xylene			His299 Tyr62 Leu165
Acarbose	3top	Asp1555 Arg1582 Asp1317 His1584 Trp1355 Thr1528 Gln1561 Lys1460 Asp1157 Met1421 Tyr1167 Arg1516 Asp1526	Tyr1251 Phe1559
Methane isocyanato		Arg1582 Asp1279 Asp1157 Asp1526 Lys1460	Phe1560 Trp1355 Tyr1251 Pro1159
p-Xylene			Phe1560 Trp1355 Phe1559 Trp1418 His1584 Tyr1251

2D/3D Interaction

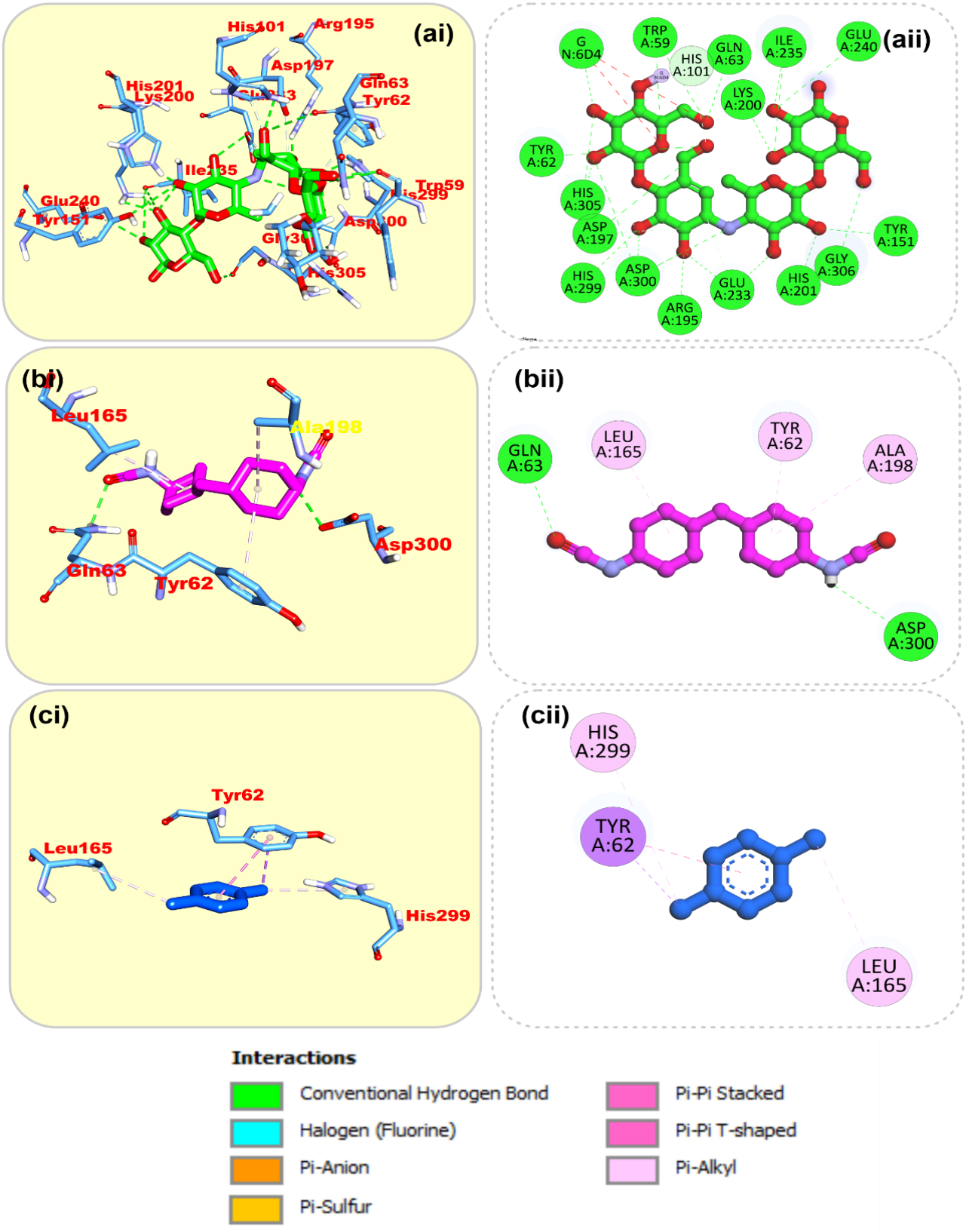

Figure 02: Top docked phytochemicals and reference inhibitor (MUP901) from the docking analysis of GCMS identified phytochemicals from methanol seed fraction of *Buccholziacoriacea* interacting with amino acids in the active site of 1LPB. The ligands are displayed as sticks (a) MUP901 (b) Methane_isocyanato (c) p_Xylene. *(i)* 3D and *(ii)* 2D interaction.

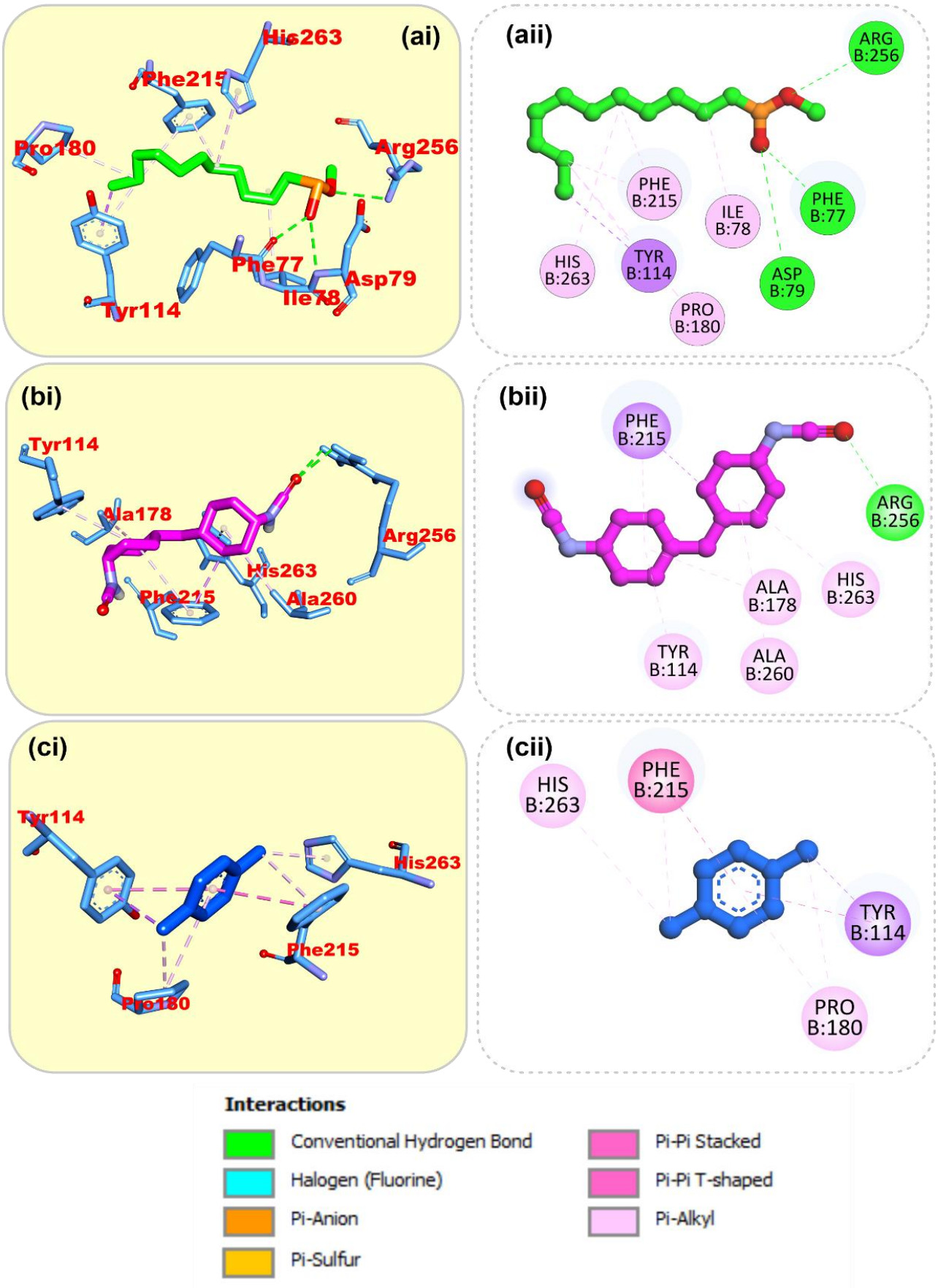

Figure 03: Top docked phytochemicals and reference inhibitor (acarbose) from the docking analysis of GCMS identified phytochemicals from methanol seeds fraction of *Buccholziacoriacea* interacting with amino acids in the active site of 1B2Y. The ligands are displayed as sticks (a)Acarbose (b) Methane_isocyanato (c) p_Xylene. *(i)*3D and *(ii)* 2Dinteraction.

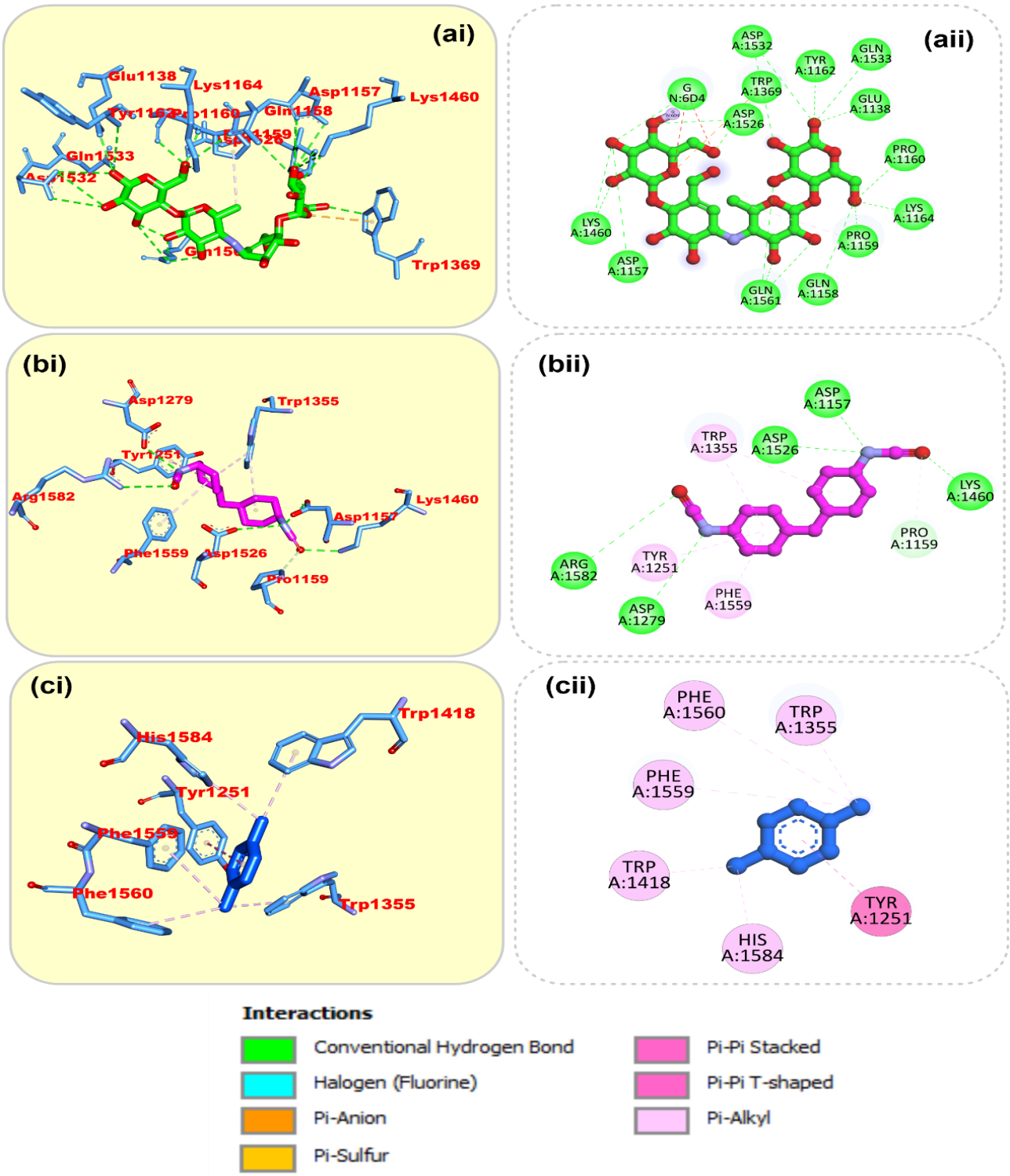

Figure 04: Top docked phytochemicals and reference inhibitor (acarbose) from the docking analysis of GCMS identified phytochemicals from methanol seeds fraction of *Buccholziacoriacea* interacting with amino acids in the active site of 3TOP. The ligands are displayed as sticks (a) Acarbose (b) Methane_isocyanato (c) p_Xylene.

DISCUSSION

There is an increased interest in alternative therapies globally and a rising increase in the use of plant derived products as they are convenient alternative or complimentary to the use of orthodox or synthetic drugs [32]. The World Health Organization reported that more than 85% of the world population, especially those residing within developing countries depends on traditional system of medicine to treat a variety of diseases [32]. *Buchholzia coriacea* seed extracts have been claimed to be efficacious in the treatment of diabetes mellitus by traditional healers in the Northern part of Nigeria.

The main organ central in the regulation of multiple physiological functions, such as removal of metabolic wastes and toxins, maintenance of electrolyte and fluid

balance, as well as homeostatic control of pH are the Kidneys. In addition, kidneys participate in systemic gluconeogenesis, production or activation of hormones[33]. Serum urea, serum albumin and serum creatinine levels are commonly employed as physiological indicators of kidney function [34]. In this study, the falling levels of these biomarkers indicate that the n-hexane, n-butanol, ethyl acetate and aqueous fractions of *B. coriacea* seeds do not possess a nephrotoxic potential at the 100mg/kg dose. This result corroborates the work of Akpotaire and Seriki whose report stated that the nephrotoxic potentials of ingested substances can be determined by measuring the levels of serum urea and serum creatinineand Lapshak *et al.* whose research observed thatno significant difference existed in the levels of Urea and creatinine in both the alloxan induced diabetic groups nor in the extract treated groups compared to the normal control group [35, 36]. The likelihood of nephrotoxicity increases with prolonged high dosage use especially in cases of high dose consumption for longer than twelve weeks.

Researchers believe oxidative stress plays a role in the onset of many chronic and degenerative conditions. Anything that raises the number of free radicals in your body to unhealthy levels can cause oxidative stress [37]. Oxidative stress parameters can be determined spectrophotometrically in plasma by measuring superoxide anion radical (O_2^-), hydrogen peroxide (H_2O_2), nitric oxide (NO) in the form of nitrites (NO_2^-) and the index of lipid peroxidation in the form of thiobarbituric acid-reactive substances (TBARS) [38]. The effect of *B. coriacea* seed fractions on super oxide dismutase, catalase, reduced glutathione, and thiobarbituric acid (TBARS) levels in normal, diabetic and fraction treated rats were assessed in this study and served as the markers for oxidative stress. Induction of diabetes was found to significantly ($p<0.05$) lower the activity of the antioxidant markers in the diabetic control group compared with the normal control. It was however noticed that the activity of the antioxidant markers which were significantly suppressed in the diabetic control was significantly ($p<0.05$) increased in the treated groups of n-hexane, n-butanol, ethyl acetate and aqueous fractions. From this result we can observe that high blood sugar levels in diabetes lead to the production of excess reactive oxygen species (ROS) which cause oxidative stress, damaging cells and tissues. Eventually, the increased ROS overwhelms the body's natural antioxidant defenses, leading to a depletion of antioxidant enzymes like SOD, CAT, and GSH which are crucial for neutralizing ROS and protecting cells from oxidative damage that leads to the development of diabetic complications such as nephropathy, neuropathy, and retinopathy. Therefore, the ability of the fractions to elevate SOD, CAT and GSH activity shows the efficacy of *B. coriacea* seed fractions in preventing the development of the listed diabetic complications by scavenging the oxidative stress biomarkers. When looking at the activity of the antioxidant marker thiobarbituric acid, it was noticed that its values were an inverse of the other markers as it was significantly ($p<0.05$) increased in the diabetic rats in comparison to the normal control, while the value of the fractions were found to have been significantly ($p<0.05$) decreased in the group treated with the n-hexane, n-butanol, ethyl acetate and aqueous treated groups when compared to the diabetic control.

Among enzymes involved in carbohydrate metabolism, Phosphofructokinase (PFK) acts as a key regulator of glycolysis, controlling the rate at which glucose is broken down to produce energy and its activity can be affected by insulin resistance and other metabolic changes in diabetes. Hexokinase is said to be responsible for initiating the first step of glucose metabolism by converting glucose to glucose-6-phosphate (G6P) which is then acted upon by glucose-6-phosphatase (G6Pase) to convert G6P to free glucose which is then released into the blood stream [39]. This enzyme G6Pase also plays an important role in the process of gluconeogenesis and glycogenolysis [40]. The activities of glucose metabolizing enzymes like hexokinase, Phosphofructokinase, Glucose-6-phosphatase and liver glycogen were significantly ($p<0.05$) lowered in the liver of diabetic untreated rats. An increase in hexokinase levels generally signifies enhanced glucose uptake and metabolism within cells. This indicates that there is an **i**ncreased utilization of Glucose showing that the body is up-regulating hexokinase to enhance glucose metabolism as a compensatory response. An increase in PFK levels generally indicates an up-regulation of glycolysis, the metabolic pathway responsible for breaking down glucose to produce energy. According to Boron and Boulpaep's Medical Physiology 3rd edition, elevated levels of glucose-6-phosphatase can be seen in conditions such as diabetes mellitus**,** where the body needs to produce more glucose to compensate for insulin resistance or deficiency [41]. An increase in liver glycogen levels generally means that the liver is storing more glucose as glycogen. The liver acts as a storage depot, converting excess glucose into glycogen for future energy needs. Elevated liver glycogen levels can also be influenced by insulin, a hormone that promotes the storage of glucose.

Molecular docking studies provide a cost-effective and time-efficient method to screen natural compounds for potential drug candidates [42]. By predicting the binding affinity and mode of interaction between plant-derived compounds and target proteins, researchers can prioritize compounds for further in vitro and in vivo testing. The interaction of the reference compound and two top-ranked GC-MS-identified phytochemicals with catalytic residues of target proteins as represented in Table 6 shows that a majority of the interactions between the ligand groups and the enzyme residues were hydrophobic, with a small number of H-bonds below 3.40Å. From the validation analysis, in a similar binding conformation as the native ligand, acarbose was stretched in the long,

narrow, hydrophobic gorge of 3TOP. Both Methane_isocyanato and Xylene made few hydrogen bonds and hydrophobic contacts with the catalytic residues at the hydrophobic gate of α-amylase which is composed of residues Trp-59, Tyr62, and His299 and other catalytic residues such as catalytic residues, including Asp197, His305, Glu233, Arg197, and Ala198. The top docked phytochemicals were docked into the active sites of 3TOP in close fashion as the reference compound acarbose and interacted with catalytic residues as acarbose. While MUP901, the native ligand of 1LPB formed 3 hydrogen bonds with Asp79, Phe77 and Arg256, a pi-sigma interaction with Tyr114, and alkyl contact with Phe215, Iler78, His263, Pro180. Methane_isocyanato also formed a hydrogen bond with Arg256, a pi-sigma contact with Phe215 and alkyl contact with Tyr114, Ala260, Ala178 and His263. Acarbose the native ligand made several hydrogen bonds with the residues of 1B2Y. Methane isocyanato-formed 2 hydrogen bonds with Gln63 and Asp300, and pi-alkyl contact with Leu165, Tyr62, and Ala198. p_xylene did not form hydrogen bonds with the residues of 1B2Y, but interacted via pi-sigma contact with Tyr62, pi-pi stacking to Tyr62 and pi-alkyl and alkyl contact with His299 and Leu165.

CONCLUSION

The molecular docking studies of methanol seed fractions of Buchholzia coriacea, guided by GC-MS analysis, revealed promising bioactive compounds with significant binding affinities to selected molecular targets. These findings, supported by both experimental and computational models, underscore the therapeutic potential of these phytochemicals, particularly in the context of drug discovery and development.

RECOMMENDATION

Further in vitroand in vivo validations are essential to confirm these compounds' biological activities and to explore their mechanisms of action, paving the way for their potential pharmaceutical applications.

REFERENCES

1. Prakash, B.; Kumar, A.; Singh, P.P.; Songachan, L.J.F. Antimicrobial and antioxidant properties of phytochemicals: Current status and future perspective. Funct. Preserv. Prop. Phytochem. **2020**, 1–45. [CrossRef]
2. Ojo, O.A.; Oni, A.I.; Grant, S.; Amanze, J.; Ojo, A.B.; Taiwo, O.A.; Maimako, R.F.; Evbuomwan, I.O.; Iyobhebhe, M.; Nwonuma, C.O. Antidiabetic Activity of Elephant Grass (Cenchrus Purpureus (Schumach.) Morrone) via Activation of PI3K/AkT Signaling Pathway, Oxidative Stress Inhibition, and Apoptosis in Wistar Rats. Front. Pharmacol. **2022**, 13, 845196. [CrossRef]
3. Obembe, O. O., Onasanwo, S. A., Raji, Y. (2012). Preliminary study on the effects of *Buchholzia coriacea* seed extract on male reproductive parameters in rats. *Niger. J. Physiol. Sci.* 2012; 27: 165–169.
4. Chinedu, F. A., Chibeze, I., Emma, E., Chukwuenweiwe, E. (2012) The phytochemical, antispasmodic and antidiarrhoea properties of the methanol extract of the leaves of *Buchholzia coriacea* family capparaceae. *Int. Journal of Curr. Pharmaceutical Res.* 2012; 4(3): 340-345. ISSN-0975-7066
5. Ajaiyeoba, E. O., Onocha, P. A., Olanrewaju. O. T. (2011) In vitro anti-helminthic properties of Buchholzia coriacea and Gynandropsis gynandra. *Pharm Biol*. 2011; 39: 217-20.
6. Mbata, T. I., Duru, C. M., Onwumelu, H. A. (2009) Antibacterial activity of crude seed extracts of Buchholzia coriacea on some pathogenic bacteria. *Journal of Dev. Biol and Tissue Eng*. 2009; 1(1): 001-005.
7. Ezekiel, O. O., Onyeoziri, N. F. (2009) Preliminary studies on the antimicrobial properties of Buchholzia coriacea. *Afr. Journal of Biotech*. 8(3):472-474.
8. Adisa, R. A., Chouhary, M. I., Olorunsogo, O. O. (2011). Hypoglycemic activity of Buchholzia coriacea (Capparaceae) seeds in streptozocin induced diabetic rats and mice. *Exp Toxicol Pathol.* 2011; 63(7-8): 619-25.
9. Theophine, C. O., Peter, A. A., Chinenye, L., Adaobi, C. E., Collins, A. O. (2012). Anti-diabetic effects of methanol extract of the seeds of Buchholzia coriacea and its synergistic effects with metformin. *Asian Journal of Biomed and Pharmaceutical Sci.* 2012; 2(12):32-36.
10. Okoli, B. J., Okere, O. S., Adeyemo, S. O. (2010). The antiplasmodial activity of Buchholzia Coriacea. *J. of Med. and Appl. Biosciences*. 2010;2:21-29.
11. Ezeja, M. I., Ezeigbo, I. I., Madubuike, K. G. (2011). Analgesic activity of the methanolic seed extract of Buchholzia coriacea. *Res J of Pharm, Biol and Chem Sci*. 2011;2(1):187-193.
12. Savych, A.; Marchyshyn, S.; Kyryliv, M.; Bekus, I. Cinnamic acid and its derivatives in the herbal mixtures and their antidiabetic activity. Farmacia **2021**, 69, 595–601. [CrossRef]
13. Global Burden of Disease. (2020). Diseases and Injuries Collaborators. Global burden of 369 diseases and injuries in 204 countries and territories, 1990–2019: a systematic analysis for the Global Burden of Disease Study 2019. *Lancet* 2020; 396: 1204–22.
14. Chan, J. C. N., Lim, L. L., Wareham, N. J., et al. (2021) The Lancet Commission on diabetes: using data to transform diabetes care and patient lives. *Lancet* 2021; 396: 2019–82.
15. International Diabetes Federation. (IDF) (2021). IDF Diabetes Atlas, 10th edition. Brussels: International Diabetes Federation, 2021.
16. Sun, H., Saeedi, P., Karuranga, S., et al. (2022) IDF Diabetes Atlas: Global, regional and country-level diabetes prevalence estimates for 2021 and

projections for 2045. *Diabetes Res Clin Pract*;183: 109119.
17. Institute for Health Metrics Evaluation, (2023). IHME news release for June 2023. https://www.healthdata.org/news-events/newsroom/news-releases/global-diabetes-cases-soar-529-million-13-billion-2050 (accessed Sep 30, 2024)
18. *Mostashari-Rad, T., Arian, R., Mehridehnavi, A., Fassihi, A. & Ghasemi, F. (2019). "Study of CXCR4 chemokine receptor inhibitors using QSPR and molecular docking methodologies".Journal of Theoretical and Computational Chemistry. 178(4). doi:*10.1142/S0219633619500184. S2CID 164985789
19. Morris, G. M., Huey, R., Lindstrom, W., Sanner, M. F., Belew, R. K., Goodsell, D. S. and Olson, A. J. (2009) 'AutoDock4 and AutoDockTools4: Automated docking with selective receptor flexibility', Journal of computational chemistry, 30(16), pp. 2785-2791.
20. Ibrahim, M. A. and Islam, M.S. (2014). Anti-diabetic effects of the acetone fraction of *Senna singueana* stem bark in a type 2 diabetes rat model. *Journal of Ethnopharmacology*, 153: 392–399.
21. O'Boyle, N. (2011) 'Banck M. James CA Morley C. Vandermeersch T. Hutchison GR Open Babel: An open chemical toolbox', J. Cheminf, 3(1), pp. 33.
22. Misra, H.P and Fridovich I. (1979).The role of superoxide anion in the antioxidant of epinephrine and simple assay for SOD. *Journal of Biological Chemistry,* 2457: 3170-3175.
23. Aebi, H. (1984). Catalase. In: *Methods in Enzymology*. Packer, L ed. Academic Press, Orlando.105: 121-126.
24. Ellman. G. L. (1959). Tissue sulfhydryl group. *Archives of Biochemistry and Biophysics*, 2: 70 – 77.
25. Okhawa, H, Ohishi, N and Yagi, K. (1979). Assay for lipid peroxides in animal tissues by thiobarbituric acid reaction. *Analytical Biochemistry,* 95 (2): 351 – 358.
26. Easterby, J.S and Qadri, S.S. (1973). Hexokinase Type II from Rat Skeletal Muscle. In:
27. King, J. (1965). *Practical Clinical Enzymology*. London: Van Nostrand, (pp 85-234).
28. Fiske, C.H., and Subbarow, Y. J. (1925). The colourimetric determination of Phosphorus. *Journal of Biological Chemistry* 66, 375-400.
29. Kaplan, L.A., Saabo, L.L and Opherin, E. K. (1988). Clinical Chemistry Interpretation and Techniques. Lea and Faerbiger, Philadelphia, USA: 1118 – 1160.
30. Ochei and Kolhatkar. (2008): *Textbook of Medical Laboratory Technology*. 3rd Edition.
31. Trott, O. and Olson, A. J. (2010) 'AutoDock Vina: improving the speed and accuracy of docking with a new scoring function, efficient optimization, and multithreading', Journal of computational chemistry, 31(2), pp. 455-461.
32. World Health Organization (2003). *Traditional Medicine*. Fact Sheet No. 134. WHO Geneva, Switzerland.
33. Imenez Silva, P. H., & Mohebbi, N. (2022). Kidney metabolism and acid-base control: back to the basics. *Pflugers Archiv : European journal of physiology*, *474*(8), 919–934. https://doi.org/10.1007/s00424-022-02696-6
34. Sakhuja, A., Chalupsky, M., & Lerma, V. (2024, May 2). Novel Biomarkers of Kidney Function Introduction and Overview. *Medscape*. Retrieved January 8, 2025, from https://emedicine.medscape.com/article/1925619-overview?form=fpf
35. Akpotaire, P. A. & Seriki, S. A. (2023) Assessment and Correlation of Serum Urea and Creatinine Levels in Normal, Hypertensive, and Diabetic Persons in Auchi, Nigeria. *Arch Pathol Clin Res*, 2023; 7: 007-016. https://doi.org/10.29328/journal.apcr.1001035
36. Lapshak, J. L., Domkat, C. L. & Nansah, S. L. (2016) The Effect of Aqueous Extract of *Buchholzia coriacea* Seeds on Some Biochemical Parametersin Normal and Alloxan-induced Diabetic Rats. *International Journal of Biochemistry Research & Review,* 11(*1*): 1-10, Article no.IJBCRR.24495, ISSN: 2231-086X.
37. Cleveland Clinic (2025). Oxidative Stress. *Cleveland clinic* Articles. Retrieved May 23, 2025, from https://my.clevelandclinic.org/health/articles/oxidative-stress
38. Djordjevic, J., Ignjatovic, V., Vukomanovic, V., Vuleta, K., Ilic, N., Slovic, Z., Stanojevic-Pirkovic, M. & Mihaljevic, O. (2024). Laboratory puzzle of oxidative stress, parameters of hemostasis and inflammation in hospitalized patients with COVID-19. *Biomedicines*, *12*(3), 636. https://doi.org/10.3390/biomedicines12030636
39. Rabbani, N., Xue, M., & Thornalley, P.J. (2022). Hexokinase-2-Linked Glycolytic Overload and Unscheduled Glycolysis—Driver of Insulin Resistance and Development of Vascular Complications of Diabetes. *International Journal of Molecular Sciences*, 23(4), 2165. https://doi.org/10.3390/ijms23042165
40. Mills, H., Acquah, R., Tang, N., Cheung, L., Klenk, S., Glassen, R., Pirson, M., Albert, A., Hoang, D. T., & Van, T. N. (2022). Type 2 Diabetes Mellitus (T2DM) and Carbohydrate Metabolism in Relation to T2DM from Endocrinology, Neurophysiology, Molecular Biology, and Biochemistry Perspectives. *Evidence-based complementary and alternative medicine: eCAM*, *2022*, 1708769. https://doi.org/10.1155/2022/1708769
41. *Boron, W. F. & Boulpaep, E. L., eds. (2017). Medical Physiology (3rd ed.). Philadelphia, PA: Elsevier.* ISBN 978-1-4557-4377-3.
42. **Natarajan, V., Harish, N., Chandan, S., & Shivaraj, K. (2023).** GC-MS Analysis and Molecular Docking Studies of an Antinephrolithiatic Compounds Identified from Stem of *Musa paradisiaca* Plantain Juice. *European Current Biology*, 302.